ChemComm

Accepted Manuscript

This article can be cited before page numbers have been issued, to do this please use: T. Wang, W. Zhu, X. Chai, B. Wang, Y. Zou, Q. Meng and Q. Wu, *Chem. Commun.*, 2015, DOI: 10.1039/C5CC02496J.

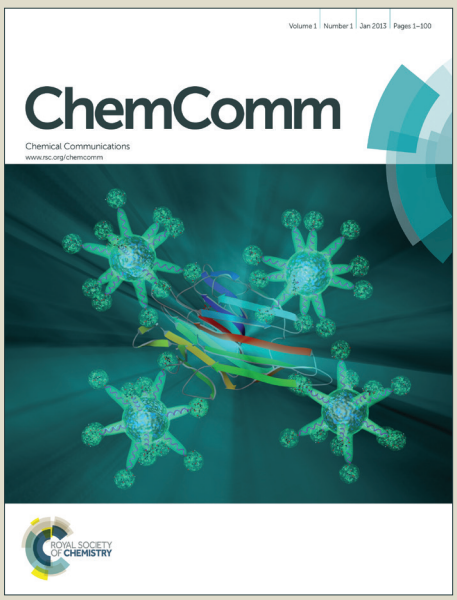

ROYAL SOCIETY OF CHEMISTRY

www.rsc.org/chemcomm

View Article Online
DOI: 10.1039/C5CC02496J

Journal Name

COMMUNICATION

Spiroboronate Si-rhodamine as a near-infrared probe for imaging lysosomes based on reversible ring-opening process

Received 00th January 20xx,
Accepted 00th January 20xx

DOI: 10.1039/x0xx00000x

www.rsc.org/

Weiwei Zhu,[ab‡] Xiaoyun Chai,[b‡] Baogang Wang,[b] Yan Zou,[b] Ting Wang,*[b] Qingguo Meng,[a] and Qiuye Wu[b]

A cyclic boronate structure was incorporated into Si-rhodamine to design a pH-activatable near-infrared (NIR) probe based on reversible ring-opening process triggered by H^+. The probe showed general suitability of specific labelling acidic lysosomes and tracking their pH changes in living cells.

Intracellular pH plays vital roles in a variety of critical cellular functions in cells and specific subcellular organelles.[1] In lysosomes, an acidic environment can serve to activate the enzyme, facilitating the degradation of proteins in cellular metabolism. Meanwhile, abnormal pH values in lysosomes often associate with cellular dysfunction.[2] Accordingly, labelling acidic organelles and tracking their pH changes are crucial for studying physiological and pathological processes. Owing to the high sensitivity and selectivity, fluorescent probes have become indispensable for monitoring pH *in vivo*.[3] In particular, design of NIR (650-900 nm) pH-activatable fluorescent probes[4] is especially preferred because NIR light minimizes photodamage and avoids the influence of autofluorescence.[5] So far, several NIR fluorescent pH probes have been developed and most of them are based on cyanine, in which the fluorescence behavior is controlled by the photoinduced electron transfer (PeT) process through the protonation/deprotonation of their amine-containing side chains. Although widely used, these NIR pH probes have some inherent deficiencies for bioimaging: firstly, in most cases cyanine-based probes easily suffer from photobleaching; additionally, sometimes the PeT process has poor efficiency, resulting in relatively high and nonspecific background signals; lastly, only a few of them work in the pH range of 5-6 and can be used for studying acidic organelles *in vivo*.[4b, 4e] Therefore, the development of new photostable NIR fluorescent pH probes with high signal/noise ratio and alternative H^+-responsive mechanism is of great significance and practical value.

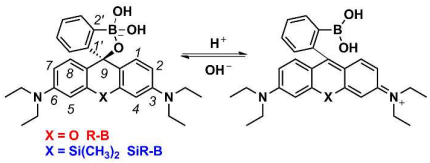

Scheme 1 Chemical structures of spiroboronate derivatives (**R-B** and **SiR-B**) and the reversible transformation between boronate and boronic acid .

Si-rhodamine (**SiR**) recently has become rather popular in the field of bioimaging because of its excellent NIR photophysical properties and biocompatible characteristics.[6] Particularly, spirocyclization of **SiR** is an attractive strategy for designing NIR fluorescent probes, as the spirocyclic **SiR** is colorless and nonfluorescent, whereas opening the corresponding spiroring gives rise to a blue color change and strong NIR fluorescence. Following the design principle, some **SiR**-based fluorescent probes have been exploited for imaging Hg^{2+},[7] ClO^-[8] and proteins of interest in living cells.[9] Although rhodamine-based pH-activatable probes have been well developed from spirolactam,[3b, 10] similar approach have yet not successfully achieved in **SiR** because of the unsatisfied spirocyclization equilibrium of spirolactam within proper pH range. Thus, new spirocyclization of **SiR** with ring-opening process that can be precisely controlled by H^+ arose our interests.

As a promising recognition group, boronic acid has attracted considerable interest owing to their unique binding and reactive abilities. A variety of boronic acid and boronate-based fluorescent probes have been developed for detecting biologically relevant species.[11] Boronic acid participates in such equilibria: in neutral or mildly basic environment, it binds with the hydroxyl groups containing substances and forms corresponding boronate which can be reversibly hydrolyzed to boronic acid in acid condition. The reversible transformation between boronate and boronic acid under external stimuli of H^+ offers a new clue to design boron-containing spirocyclic derivatives based on rhodamine and **SiR** (Scheme 1). Herein we designed and synthesized a **SiR**-based spirocyclic derivative **SiR-B**, in which a boronic acid group was introduced to replace the carboxyl group at 2' position. Meanwhile, its rhodamine analogue **R-B** was also prepared as a comparison. To

[a] College of Pharmacy, Yantai University, Yantai, Shandong 264005 (China).
[b] Department of Organic Chemistry, College of Pharmacy, Second Military Medical University, Shanghai 200433 (China).
‡ W. Zhu and X. Chai contributed equally to this work.
E-mail: wangting1983928@gmail.com
†Electronic Supplementary Information (ESI) available: general methods, synthesis, optical properties and confocal microscopy studies. See DOI: 10.1039/x0xx00000x

View Article Online
DOI: 10.1039/C5CC02496J

the best of our knowledge, this is the first example of the spiroboronate ring in rhodamine and **SiR** systems. Probes **SiR-B** and **R-B** both displayed the reversible H^+-triggered ring-opening process of the corresponding spirocylic structures accompanied by remarkable chromogenic and fluorogenic changes. Furthermore, probe **SiR-B** showed abrupt fluorescence change in the pH range from 7.4 to 5.0, demonstrating ideal suitability for specific labelling acidic lysosomes and tracking their pH changes in living cells.

As presented in Scheme 2, probe **SiR-B** was synthesized by addition of a lithiated benzene moiety bearing a protected boronic acid group to Si-containing xanthone (**SiX**),[7, 8] followed by deprotection in hydrochloric acid (HCl) solution. In the protection of boronic acid group, N-butyldiethanolamine was chosen as a protective reagent because of its tolerance to lithiation and effective deprotection.[12] However, a similar synthetic approach has failed in synthesizing probe **R-B**. **R-B** was obtained from iodine-substituted rosamine *via* coupling reaction and subsequent deprotection reaction. The structures of probes **SiR-B** and **R-B** were confirmed by high-resolution mass spectrometry and NMR spectroscopy.

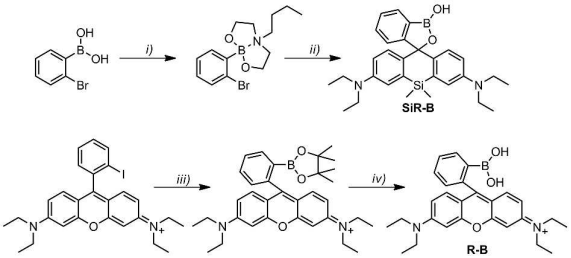

Scheme 2 Synthesis of probes **SiR-B** (i and ii) and **R-B** (iii and iv). Conditions: *i*) N-butyldiethanolamine, PhMe, 50 °C; *ii*) *n*-BuLi, THF,–78 °C, then compound **SiX**, THF, –78 °C to r.t., then 6M HCl, r.t.; *iii*) Bis(pinacolato)diboron, $PdCl_2(dppf)_2$, KOAc, DMSO, 80 °C; *iv*) BBr_3, CH_2Cl_2, 0 °C.

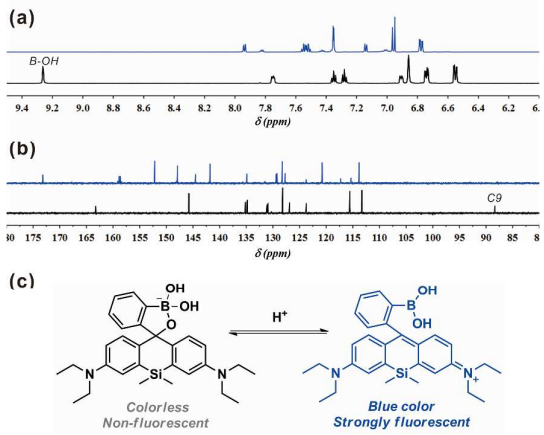

Fig. 1 (a) and (b) ^1H and ^{13}C NMR spectral changes of probe **SiR-B** upon addition of 1.5 equiv. of CF_3COOD (black lines: before adding CF_3COOD; blue lines: after adding CF_3COOD). (c) Proposed H^+-responsive mechanism based on the ring-opening process of spiroboronate in SiR-B.

The probe **SiR-B** formed colorless solution in most aprotic organic solvents, but underwent a reversible blue color change after adding AcOH or Et_3N (Fig. S1, ESI†). Correspondingly, a bright pink color was observed in initial probe **R-B** solution and similar H^+-dependent color response was observed. These phenomena implied that the boron-containing groups in both probes **SiR-B** and **R-B** are sensitive to H^+, and the reversible color changes is likely to be induced by the reversible ring-opening process of the corresponding rings. To fully explore the H^+-responsive mechanism, we compared the NMR spectral changes of probe **SiR-B** upon addition of H^+ (Fig. 1). In DMSO-d_6, a singlet resonating at δ = 9.26 ppm in ^1H NMR could be assigned to the B-OH and the signal resonating at δ = 88 ppm in ^{13}C NMR corresponds to the quaternary carbon atom at position 9 (*C9*).[13] These characteristic peaks indicated that probe **SiR-B** existed predominantly in its spirocyclic form in aprotic organic solvents. After adding H^+, the B-OH signal dismissed, suggesting the interaction between spiroboronate and H^+. Meanwhile, no such signal of the quaternary carbon at similar region was observed. The significant upfield shift of the *C9* signal directly confirmed the ring-opening of the spiroboronate in probe **SiR-B** by formation of boronic acid.

The pH-dependent spectral properties of probes **SiR-B** and **R-B** were further evaluated in phosphate buffer solution (containing 1% DMSO). As shown in Fig. S2 (ESI†), free **SiR-B** was colorless and almost nonfluorescent at physiological pH of 7.4 as a result of the intermolecular spirocyclization. When the pH decreased from 7.4 to 5.0, the solution changed to blue color with appearing and dramatically increasing of an intense band at 664 nm. Concomitantly, the fluorescence at 680 nm was significantly enhanced with a 20-fold intensity increase within the studied pH range duo to the ring-opening process of spiroboronate. At pH 5.5, probe **SiR-B** existed in the ring-opening form with maximum fluorescence, possessing an extinction coefficient of 105000 M^{-1} cm^{-1} and a fluorescence quantum yield of 0.31 (Table 1). The fluorescence pH titration curve of probe **SiR-B** yielded pK_{cycl} (equilibrium constant of intramolecular spirocyclization) of 6.2,

Table 1 Photochemical Properties of Probes **SiR-B** and **R-B**

Probes	λ_{abs}/nm	λ_{em}/nm	ε/M^{-1} cm^{-1}	Φ^c	$pK_{cycl}{}^d$
SiR-B[a]	651	667	105000	0.31	6.2
R-B[b]	555	576	101000	0.33	9.6

[a]Measured in phosphate buffer (pH = 5.5) containing 1% DMSO. [b] Measured in phosphate buffer (pH = 7.4) containing 1% DMSO. [c]Cy5 (Φ = 0.27, PBS) and Rhodamine B (Φ = 0.31, water) were used as the references for the fluorescence quantum yields of probes **SiR-B** and **R-B**, respectively. [d]Calculated from fluorescence pH titration.

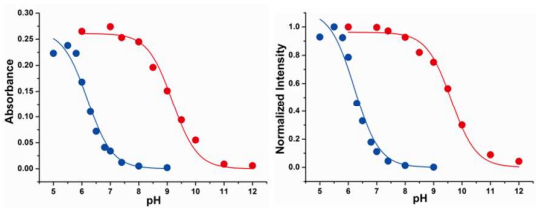

Fig. 2 Absorbance and fluorescence pH titration curves of probes **SiR-B** (blue, λ_{abs} = 651 nm, λ_{ex} = 620 nm, λ_{em} = 667 nm) and **R-B** (red, λ_{abs} = 555 nm, λ_{ex} = 520 nm, λ_{em} = 576 nm).

View Article Online
DOI: 10.1039/C5CC02496J

suggesting that probe **SiR-B** may serve as an appropriate NIR pH probe for imaging acidic pH *in vivo*. By sharp contrast, probe **R-B** solution displayed a pink color (ε = 101000 M^{-1} cm^{-1}) and strong fluorescence (Φ = 0.33) at pH 7.4, suggesting that probe **R-B** preferred the ring-opening form at physiological pH. As the pH increased to 12.0, the intermolecular spirocyclization of boronic acid resulted in the immediately fading of the absorption and fluorescence intensity (Fig. S3, ESI†). The pK_{cycl} value of probe **R-B** was 9.6, which was much higher than that of probe **SiR-B**. The comparison of two pH-activatable probes revealed that they shared similar pH-dependent ring-opening process of corresponding spiroboronate accompanied with chromogenic and fluorogenic changes. The intriguing difference of intramolecular spirocyclization behavior was likely to attribute to the different stability of spiroring as suggested by us and other research groups.[7, 9] Strong electrophilicity of the **SiR** fluorophore stabilized the spirocyclic structure, thereby shifting the pK_{cycl} value to acidic pH region. The exceptional photophysical characteristics and H^+-responsive behavior of probe **SiR-B** ensure that it is a promising candidate for imaging pH *in vivo*, especially labelling and tracking acidic lysosomes which can reach pH value as low as ~5.

The properties of probe **SiR-B** were scrupulously evaluated (Fig. S4-8, ESI†). Reversibility is highly required for tracking pH changes in living cells. After five cycles, no noticeable changes in the emission were observed in **SiR-B**. Meanwhile, the color of probe **SiR-B** changed repeatedly between colorless and blue. The selectivity of probe **SiR-B** to H^+ over biologically relevant species at pH 7.4 and pH 5.5 was evaluated as well. High concentrations of ions, such as K^+, Na^+, Ca^{2+}, Mg^{2+}, Cu^{2+}, Zn^{2+}, Fe^{3+} and F^- did not cause any significant fluorescence intensity changes. Other biologically important species, including amino acids and carbohydrates, caused no visible effect on the fluorescence signals. Low concentration of H_2O_2 has little influence on the emission, although very high concentration of H_2O_2 quenched the fluorescence of probe **SiR-B** at pH = 5.5. Like other **SiR**s, probe **SiR-B** was highly stable at pH of 7.4 and 5.5, showing remarkably resistance to photobleaching after irradiation.[14] Additionally, MTT assays revealed that the cell viabilities of HepG2 cells were not seriously affected by incubation with 1~10 μM probe **SiR-B** for 24 h.

As stated above, the pH-activatable probe **SiR-B** possesses excellent NIR photophysical properties with high molar extinction coefficient and high fluorescence quantum yield. In addition, it meets the requirements for imaging pH *in vivo*, such as reversibility, promising specificity, high photostability and low bio-toxicity. To evaluate the feasibility of imaging pH in living cells with probe **SiR-B**, it was employed to stain HepG2 and PC12 cells. Confocal fluorescence microscopy results showed that probe **SiR-B** accumulated into specific subcellular organelles, giving red fluorescence spots dispersed in cells. Co-staining with commercially available lysosome-specific probe LysoTracker Green DND-26 was performed to further confirm the subcellular location (Fig. 3). The yellow merged images indicated that the staining of probe **SiR-B** fit well with that of LysoTracker Green DND-26 (Fig. S9, ESI†). These results thus demonstrated that the probe **SiR-B** possessed great cell membrane permeability and general suitability of specific labelling acidic lysosomes in living cells. The efficient lysosome-targeting location of **SiR-B** without intentionally functionalized lysosome-

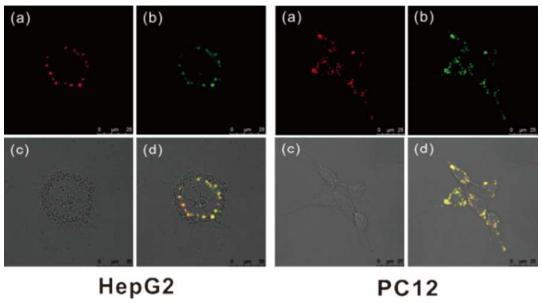

Fig. 3 Fluorescence images of HepG2 (left) and PC12 (right) cells co-stained with 5.0 μM **SiR-B** and 1 μM LysoTracker Green DND-26. (a) Fluorescence microscopic images (red channel) from probe SiR-B. (b) Fluorescence microscopic images (green channel) from LysoTracker Green DND-26. (c) Bright-field microscopic images. (d) Merged fluorescence microscopic images of green and red channels.

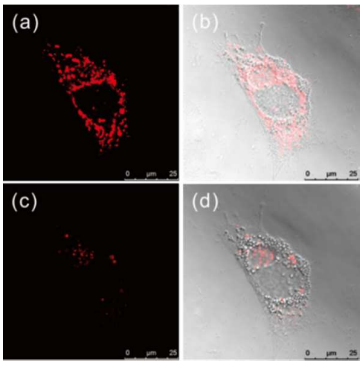

Fig. 4 Fluorescence images of probe 5.0 μM **SiR-B** in HepG2 cells stimulated with chloroquine. (a) and (b) Images of the stained cells before chloroquine stimulation; (c) and (d) Images of cells in exposed to 100 μM chloroquine for 2 min.

locating group was attributed to the H^+-triggered ring-opening process with appropriate pK_{cycl} that matched well with pH of the acidic lysosomes. The sensitive H^+-response behavior offered enhanced lysosome-specific NIR fluorescence imaging with minimal background fluorescence. Furthermore, we examined the feasibility of applying our probe for tracking the pH changes in lysosomes (Fig. 4). Obvious quenching of the fluorescence signal in the area of the lysosomes was observed after treating with chloroquine, which is commonly used in inducing an increase in the lysosomal pH. The results suggested that probe **SiR-B** could be used for tracking pH changes in lysosomes.

In conclusion, we incorporated cyclic boronate structure into rhodamine and **SiR** systems and successfully synthesized both spiroboronate rhodamine (**R-B**) and Si-rhodamine (**SiR-B**). The controlled spirocyclization of boronate in **SiR-B** generated a pH-activatable NIR probe based on reversible ring-opening process triggered by H^+. We proved that probe **SiR-B** existed as a closed spirocyclic structure in aqueous solution at physiological pH 7.4, whereas converting the spirocyclic structure to the strongly fluorescent open form at pH ~5. Taking advantage of the applicative H^+-responsive behavior and exceptional biocompatible characteristics, probe **SiR-B** showed the general suitability of specific labelling acidic lysosomes and tracking their pH changes.

View Article Online
DOI: 10.1039/C5CC02496J

These results remind us that spirocyclization of **SiR** is a powerful design strategy for designing NIR fluorescent probes in which the equilibrium between the spirocyclic closed form (colorless and nonfluorescent) and the open form (strongly fluorescent) can be precisely controlled to facilitate various applications.

This work has been supported by the National Natural Science Foundation of China (No. 21205135). We also sincerely appreciate Xiaoyan Cui for her useful discussion and suggestion.

Notes and references

1 J. R. Casey, S. Grinstein and J. Orlowski, *Nat. Rev. Mol. Cell Biol.*, 2010, **11**, 50.
2 (a) E. J. Blott and G. M. Griffiths, *Nat. Rev. Mol. Cell Biol.*, 2002, **3**, 122; (b) J. Stinchcombe, G. Bossi and G. M. Griffiths, *Science*, 2004, **305**, 55; (c) J. P. Luzio, P. R. Pryor and N. A. Bright, *Nat. Rev. Mol. Cell Biol.*, 2007, **8**, 622.
3 (a) R. Wang, C. Yu, F. Yu and L. Chen, *TrAC-Trend. Anal. Chem.*, 2010, **29**, 1004; (b) H. Zhu, J. Fan, Q. Xu, H. Li, J. Wang, P. Gao and X. Peng, *Chem. Commun.*, 2012, **48**, 11766; (c) H. J. Kim, C. H. Heo and H. M. Kim, *J. Am. Chem. Soc.*, 2013, **135**, 17969; (d) G. Li, D. Zhu, L. Xue and H. Jiang, *Org. Lett.*, 2013, **15**, 5020.
4 (a) Z. R. Zhang and S. Achilefu, *Chem. Commun.*, 2005, 5887; (b) S. A. Hilderbrand and R. Weissleder, *Chem. Commun.*, 2007, 2747; (c) B. Tang, F. Yu, P. Li, L. L. Tong, X. Duan, T. Xie and X. Wang, *J. Am. Chem. Soc.*, 2009, **131**, 3016; (d) H. Lee, W. Akers, K. Bhushan, S. Bloch, G. Sudlow, R. Tang and S. Achilefu, *Bioconjugate Chem.*, 2011, **22**, 777; (e) T. Myochin, K. Kiyose, K. Hanaoka, H. Kojima, T. Terai and T. Nagano, *J. Am. Chem. Soc.*, 2011, **133**, 3401; (f) L. Fan, Y. J. Fu, Q. L. Liu, D. T. Lu, C. Dong and S. M. Shuang, *Chem. Commun.*, 2012, **48**, 11202; (g) W. Liu, R. Sun, J.-F. Ge, Y.-J. Xu, Y. Xu, J.-M. Lu, I. Itoh and M. Ihara, *Anal. Chem.*, 2013, **85**, 7419; (h) Q. Wan, S. Chen, W. Shi, L. Li, H. Ma, *Angew. Chem., Int. Ed.*, 2014, **53**, 10916; (i) D.-D. He, W. Liu, R. Sun, C. Fan, Y.-J. Xu and J.-F. Ge, *Anal. Chem.*, 2015, **87**, 1499. (j) L. Yuan, W. Y. Lin, Y. T. Yang and H. Chen, *J. Am. Chem. Soc.*, 2012, **134**, 1200.
5 (a) L. Yuan, W. Y. Lin, K. B. Zheng, L. W. He and W. M. Huang, *Chem. Soc. Rev.*, 2013, **42**, 622; (b) Z. Guo, S. Park, J. Yoon and I. Shin, *Chem. Soc. Rev.*, 2014, **43**, 16.
6 Y. Kushida, T. Nagano and K. Hanaoka, *Analyst*, 2015, **140**, 685.
7 T. Wang, Q.-J. Zhao, H.-G. Hu, S.-C. Yu, X. Liu, L. Liu and Q.-Y. Wu, *Chem. Commun.*, 2012, **48**, 8781.
8 Y. Koide, Y. Urano, K. Hanaoka, T. Terai and T. Nagano, *J. Am. Chem. Soc.*, 2011, **133**, 5680.
9 (a) G. Lukinavičius, K. Umezawa, N. Olivier, A. Honigmann, G. Yang, T. Plass, V. Mueller, L. Reymond, I. R. Corrêa Jr, Z.-G. Luo, C. Schultz, E. A. Lemke, P. Heppenstall, C. Eggeling, S. Manley and K. Johnsson, *Nat. Chem.*, 2013, **5**, 132; (b) G. Lukinavicius, L. Reymond, E. D'Este, A. Masharina, F. Gottfert, H. Ta, A. Guther, M. Fournier, S. Rizzo, H. Waldmann, C. Blaukopf, C. Sommer, D. W. Gerlich, H.-D. Arndt, S. W. Hell and K. Johnsson, *Nat. Meth.*, 2014, **11**, 731; (c) S.-n. Uno, M. Kamiya, T. Yoshihara, K. Sugawara, K. Okabe, M. C. Tarhan, H. Fujita, T. Funatsu, Y. Okada, S. Tobita and Y. Urano, *Nat. Chem.*, 2014, **6**, 681.
10 (a) L. Yuan, W. Y. Lin and Y. M. Feng, *Org. Biomol. Chem.*, 2011, **9**, 1723; (b) X.-L. Shi, G.-J. Mao, X.-B. Zhang, H.-W. Liu, Y.-J. Gong, Y.-X. Wu, L.-Y. Zhou, J. Zhang and W. Tan, *Talanta*, 2014, **130**, 356.
11 (a) E. Galbraith and T. D. James, Chem. Soc. Rev., 2010, 39, 3831; (b) Z. Q. Guo, I. Shin and J. Yoon, *Chem. Commun.*, 2012, **48**, 5956.
12 J. W. Tomsho, A. Pal, D. G. Hall and S. J. Benkovic, *ACS Med. Chem. Lett.*, 2012, **3**, 48.
13 B. Wang, X. Chai, W. Zhu, T. Wang and Q. Wu, *Chem. Commun.*, 2014, **50**, 14374.
14 Y. Koide, Y. Urano, K. Hanaoka, T. Terai, and T. Nagano, *ACS Chem. Biol.* 2011, **6**, 600-608.